

# Zirconium and hafnium permethylpentalene compounds

F. Mark Chadwick, Robert T. Cooper, Dermot O'Hare\*

Chemistry Research Laboratory, Department of Chemistry, University of Oxford, 12 Mansfield Road, Oxford, OX1 3TA, U.K.

Supporting Information Placeholder

**ABSTRACT:** A selection of new  $\eta^8$ -permethylpentalene zirconium and hafnium complexes are reported. The first d-block metal bis(permethylpentalene) sandwich complexes,  $(\text{Pn}^*_2\text{M})$  ( $\text{Pn}^* = \text{C}_8\text{Me}_6$ ;  $\text{M} = \text{Zr}, \text{Hf}$ ) have been synthesized and structurally characterized. The bis-allyl species,  $\text{Pn}^*\text{M}(\text{C}_3\text{H}_5)_2$  ( $\text{M} = \text{Zr}, \text{Hf}$ ) have been synthesized, these complexes are fluxional in solution and react with  $\text{CO}_2$  to give the double insertion product  $\text{Pn}^*\text{M}(\kappa^2\text{-O}_2\text{CCH}_2\text{CHCH}_2)_2$  ( $\text{M} = \text{Zr}, \text{Hf}$ ). We also report mono, bimetallic and polymeric  $\sigma$ -bonded alkyl derivatives such as  $(\text{Pn}^*\text{Zr})_2(\mu\text{-CH}_2)(\mu\text{-Me})_2$ ,  $\text{Pn}^*\text{Hf}(\text{CH}_2\text{Ph})_3$  and  $[\text{Pn}^*\text{ZrPh}(\mu\text{-Ph})_2\text{Li}(\mu\text{-1,4-dioxane})]_n$ .

## INTRODUCTION

Pentalene ( $\text{Pn}$ ;  $\text{C}_8\text{H}_6$ ) is a bicyclic carbocycle related to two cyclopentadiene ( $\text{Cp}$ ) units by a ring-fusion and to cyclooctatetraene ( $\text{COT}$ ) by a 1,5-transannular bond.<sup>1</sup>  $\text{COT}$  and  $\text{Pn}$  are isoelectronic. However  $\text{Pn}$  is constrained by its bridgehead bond, forcing a near planar geometry, and is therefore anti-aromatic by Hückel's  $4n$  definition. Katz *et al.* proposed, in a manner analogous to  $\text{COT}$ , that a two electron reduction of  $\text{Pn}$  could furnish a  $10\pi$  electron aromatic dianion, which would serve as an exciting precursor and ligand in organometallic chemistry.<sup>2,3</sup> The ligand can bind in a multitude of hapticities here our interest was focused on the  $\eta^8$ -bonding mode, whereby the pentalene framework wraps around a metal center and caps off one face of the metal's coordination sphere. In this instance the ligand can be thought of as mimicking two  $\text{Cp}$  moieties, however contributing two fewer electrons to the total electron count of the complex.<sup>4</sup>

The  $\eta^8$ -bonding mode was first observed by Cloke and coworkers using a substituted pentalene derivative on a tantalum center. The trichloride  $(\eta^8\text{-Pn}^{\text{R}})\text{TaCl}_3$  ( $\text{R} = 1,4\text{-SiMe}_3$ ) was initially isolated which was found to undergo sequential methylation.<sup>5,6</sup> Simultaneously, Jonas and coworkers synthesized group 4  $\eta^8\text{-Pn}$  compounds.<sup>7</sup> Treatment of  $\text{CpTiCl}_2$  with the pentalene dianion gave  $(\eta^8\text{-Pn})\text{TiCp}$ , which could subsequently be oxidized by half an equivalent of 1,2-dichloroethane to  $(\eta^8\text{-Pn})\text{TiCpCl}$ . The zirconium congener was synthesized by the direct combination of  $\text{Cp}_2\text{ZrCl}_2$  and  $\text{Li}_2\text{Pn}$ . Reaction with a further equivalent of the pentalene synthon gave the intriguing  $(\eta^8\text{-Pn})_2\text{Zr}$  species, though no structure was reported.

The progress of pentalene organometallic chemistry was initially stunted by the lack of facile syntheses of starting materials, with routes plagued by either low yields/poor purity, or the requirement for specialized equipment.<sup>8</sup> However, in 2005, Ashley and co-workers reported a homogenous, high yielding synthesis of suitable precursors for permethylpentalene ( $\text{Pn}^*$ ;  $\text{C}_8\text{Me}_6$ )<sup>9,10</sup> and this ligand has been subsequently used in early d-block and f-block organometallic chemistry.<sup>11–13</sup> Recently we reported the synthesis of  $(\eta^8\text{-Pn}^*)\text{MX}_2$  ( $\text{M} = \text{Ti}, \text{Zr}, \text{Hf}$ )

synthons,<sup>14</sup> which we used to make mixed sandwich complexes that demonstrate very high activity for  $\alpha$ -olefin polymerization. Other group four metal pentalene complexes have shown fascinating reactivity: a Ti 'super-sandwich'  $(\mu\text{-}\eta^5\text{-}\eta^5\text{-Pn}^{\text{R}})\text{Ti}_2$  [ $\text{R} = 1,4\text{-(Si}^i\text{Pr}_3)_2$ ] can reductively deoxygenate  $\text{CO}_2$  to form a dicarbonyl complex,<sup>15</sup> and, more recently, ' $\text{Pn}^*\text{Ti}$ ' complexes have shown curious insertion chemistry with  $\text{CO}_2$ .<sup>16,17</sup> Here we report the synthesis of a series of zirconium and hafnium  $\text{Pn}^*$  complexes, such as  $\text{Pn}^*_2\text{M}$  ( $\text{M} = \text{Zr}, \text{Hf}$ ),  $(\text{Pn}^*\text{Zr})_2(\mu\text{-CH}_2)(\mu\text{-Me})_2$ ,  $[\text{Pn}^*\text{Hf}(\text{CH}_2\text{Ph})_3]^-$  and  $[\text{Pn}^*\text{ZrPh}(\mu\text{-Ph})_2\text{Li}(\mu\text{-1,4-dioxane})]_n$ .

## RESULTS AND DISCUSSION

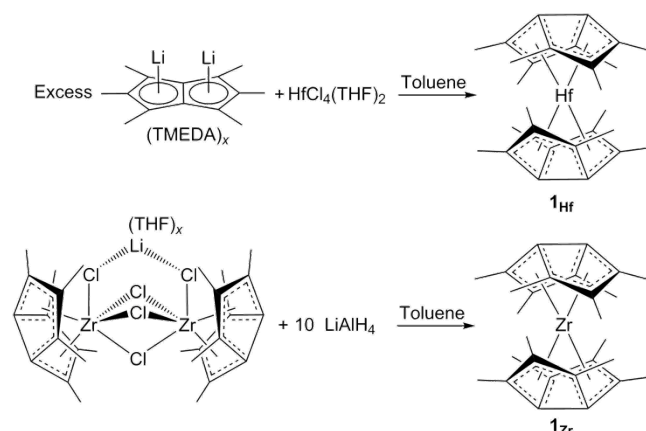
### Synthesis of $\text{Pn}^*_2\text{M}$ ( $\text{M} = \text{Zr}, \text{Hf}$ )

The earliest reports of  $\eta^8\text{-Pn}$  binding to early d-block metals involved the reports of the homoleptic bis(pentalene) species  $[(\eta^8\text{-Pn}^{\text{R}})_2\text{M}]$ , ( $\text{M} = \text{Ti}, \text{Zr}, \text{Hf}$ ,  $\text{R} = \text{H}, 2\text{-Me}$ ).<sup>7</sup> Unfortunately none of these complexes could be structurally characterized so the nature of the bonding, and in particular, the question of the total count of 20 electrons could not be structurally investigated. This prompted numerous theoretical DFT, PES, geometry optimization and symmetry studies on these species.<sup>1,18–20</sup> Consequently, the syntheses and structural elucidation of the  $\text{Pn}^*_2\text{M}$  ( $\text{M} = \text{Zr}, \text{Hf}$ ) would therefore be of great interest, especially due to the high symmetry and high steric demand of the ligand. It was also hoped that permethylation of the rings would assist in the isolation and crystallization of these complexes.<sup>21</sup>

The synthesis of  $\text{Pn}^*_2\text{Zr}$  (**1<sub>Zr</sub>**) was initially targeted via the combination of  $[\text{Pn}^*\text{Zr}(\mu\text{-Cl})_{3/2}(\mu\text{-Cl})_2\text{Li}(\text{THF})_x(\text{Et}_2\text{O})_y]$  (**A<sub>Zr</sub>**) with an excess of  $\text{Li}_2\text{Pn}^*(\text{TMEDA})_x$  in a variety of solvents, however, this approach gave no discernable reaction products, even with prolonged heating. As a result, it was initially thought the synthesis of  $\text{Pn}^*_2\text{Zr}$  (**1<sub>Zr</sub>**) was unachievable due to extreme steric crowding. However, we later found that reaction of **A<sub>Zr</sub>** with  $\text{LiAlH}_4$  yielded **1<sub>Zr</sub>**, albeit in poor yield (Scheme 1). In contrast, the synthesis of  $\text{Pn}^*_2\text{Hf}$  (**1<sub>Hf</sub>**) was relatively straight forward, by the direct combination of

HfCl<sub>4</sub>·2THF with excess Li<sub>2</sub>Pn\*(TMEDA)<sub>x</sub> and subsequent heating furnishing **1<sub>Hf</sub>** as a red solid (Scheme 1).

**Scheme 1. The synthesis of **1<sub>M</sub>** (M = Zr, Hf).**



Single crystals of **1<sub>M</sub>** (M = Zr, Hf) were grown by the slow evaporation of a concentrated solution under an inert atmosphere, yielding red crystals. **1<sub>Zr</sub>** crystallizes in the P-1 space group, with four molecules in the asymmetric unit of the unit cell whereas **1<sub>Hf</sub>** crystallizes in the C222 space group. A view of **1<sub>Zr</sub>** is shown in Figure 1.

Due to the quality of the crystallographic data, only tentative conclusions may be drawn. It is noteworthy that unlike the previously synthesized Pn\*<sub>2</sub>M (M = U, Ce) the Pn\* rings are not disordered over three positions, presumably due to the smaller size of the central metal atom locking the ligand conformation. The average M-Ct distance is greater than those reported in previously reported group 4 Pn\* complexes [distances of previously synthesized compounds range from 2.080(2)-2.135(1) Å].<sup>14,16</sup> This is thought to arise from the greater steric demand of two Pn\* ligands preventing closer approach to the metal center.

Of particular interest is the comparison of geometries found and those predicted by DFT *ab-initio* calculations, a selection of bond lengths and angles are presented in Table 1.

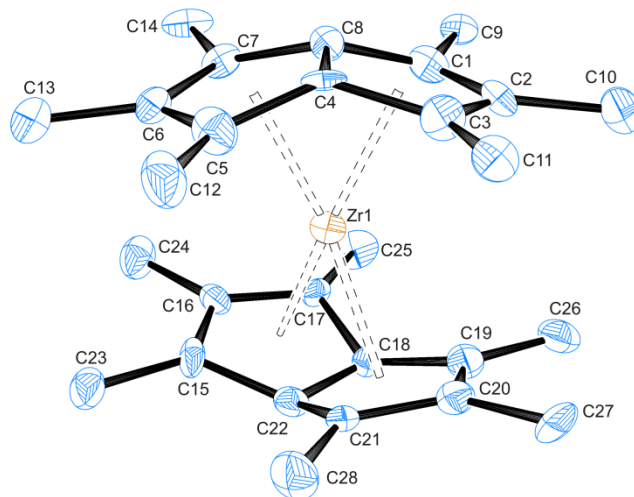


Figure 1: The solid state molecular structure of **1<sub>Zr</sub>**. Thermal ellipsoids at 50% probability and H-atoms omitted for clarity. Selected distances (Å) and angles (°) for **1<sub>Zr</sub>**: Zr1-Ct1, 2.152(7); Zr1-Ct2, 2.185(7); Zr1-Ct3 2.123(7); Zr1-Ct4 2.135(7); fold angles 24.4(8), 27.3(10), torsion angle between C6-Zr1-C2 plane and C16-Zr1-C20 plane 41.6 (5). Selected distances (Å) and angles (°) for **1<sub>Hf</sub>**: Hf1-Ct1, 2.138(5); Hf1-Ct2, 2.122(6); Hf1-Ct3 2.114(6); Hf1-Ct4 2.128(5); fold angles 27.2(10), 26.1(10), torsion angle between C6-Hf1-C2 plane and C16-Hf1-C20 plane 42.8(6). Throughout this paper Ct1 is the centroid of the C1-C2-C3-C4-C8 ring, Ct2 is the centroid of the C4-C5-C6-C7-C8 ring. Fold angle is defined as the angle between the C2 the middle of the C4/C8 bond, and C6. Ct3 is the centroid of C15-C16-C17-C18-C22 ring, Ct4 is the centroid of C18-C19-C20-C21-C22 ring.

**Table 1. Comparison of calculated and found bond lengths and angles. C<sub>BH</sub> are the bridgehead (BH) carbons, C4 and C8.**

Species	Average M-C <sub>BH</sub> (Å)	Average fold angle (°)	Torsion angle (°)
<b>1<sub>Zr</sub></b>	2.30(1)	26.0(11)	41.6(5)
(η <sup>8</sup> -Pn) <sub>2</sub> Zr	2.34	27.7	50.6
<b>1<sub>Hf</sub></b>	2.27(1)	26.7(11)	42.8(6)
(η <sup>8</sup> -Pn) <sub>2</sub> Hf	2.32	28.9	49.3

Despite the extra inductive effect of the methyl groups on Pn\* the predicted distances within the carbon skeleton of Pn<sub>2</sub>Zr agree extremely well with those found for **1<sub>Zr</sub>**, as does the predicted degree of folding of the pentalene ligand, however the fold angles have considerable uncertainty and therefore no conclusions should be drawn upon them. The greatest difference between calculation and experiment is seen in the torsion angle between the Pn\* ligands [defined as the angle between the planes made up between the wingtip (WT, C2/C6) carbons and the metal center on each Pn\* moiety], where calculations predict the pentalene rings to be more staggered than observed. This can be explained by the extra steric bulk of the Pn\* ligand compared to the non-substituted analogue, in particular the steric clash of the methyl group on the WT position, with the bridgehead (BH, C4/C8) carbon on the other pentalene ligand. It is expected this would move the energetic minimum of the HOMO to a lower torsion angle. **1<sub>M</sub>** (M = Zr, Hf) are formally 20 electron complexes. The two highest energy electrons would therefore be expected to be found in an anti-bonding orbital, however the previously mentioned DFT

study found the HOMO of the  $\text{Pn}_2\text{M}$  species to be purely localized on the Pn framework.  $\mathbf{1}_\text{M}$  could be expected to have a HOMO of similar make-up as  $\text{Pn}_2\text{M}$  and as such the slight lengthening in the M-Pn\* distances compared to other species reported (*vide infra*) is attributed to steric factors.

Both  $\mathbf{1}_\text{Zr}$  and  $\mathbf{1}_\text{Hf}$  exhibit very simple room temperature  $^1\text{H}$  NMR spectra revealing two sharp resonances in a 24:12 ratio. This implies that the Pn\* ligands can easily oscillate from the torsion angle minima and thus all the non wing tip (NWT) NWT-Me protons are equivalent at room temperature.  $\mathbf{1}_\text{Zr}$  and  $\mathbf{1}_\text{Hf}$  were also characterized by high resolution mass spectrometry revealing signals at  $m/z = 462.1864$  ( $\mathbf{1}_\text{Zr}$ ) and 552.2288 ( $\mathbf{1}_\text{Hf}$ ), and the subsequent fragmentation of the loss of Pn\* from the molecular ion.

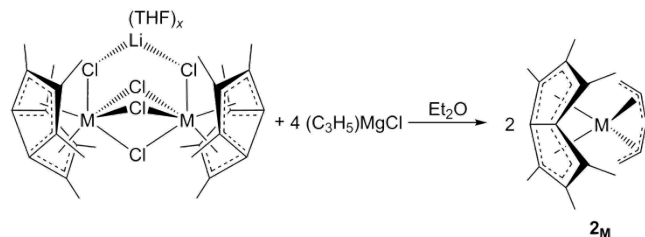
### Synthesis of $\text{Pn}^*\text{M}(\text{allyl})_2$ (M = Zr, Hf)

Organometallic complexes containing the allyl ligand ( $\text{C}_3\text{H}_5$ ) often exhibit varied hapticity, fluxional behavior and have use in the polymerization of  $\alpha$ -olefins.<sup>22–24</sup> Group 4 metal allyl complexes are however often thermally unstable, which has hampered their isolation and characterization, especially in the solid state. Despite this thermal instability,  $\text{Cp}_2\text{Zr}(\text{C}_3\text{H}_5)_2$  was synthesized by the reaction of  $\text{Cp}_2\text{ZrCl}_2$  with  $\text{C}_3\text{H}_5\text{MgCl}$ .<sup>25</sup> It was found that the allyl ligands were fluxional at room temperature, with no observed decoalescence of the  $^1\text{H}$  NMR resonances even when cooled to  $-90^\circ\text{C}$ . IR spectroscopy indicated however, that the structure contained mixed hapticity allyl ligands, and so an 18-electron formula of  $\text{Cp}_2\text{Zr}(\eta^3\text{-C}_3\text{H}_5)(\eta^1\text{-C}_3\text{H}_5)$  was assigned.

One of the earliest  $\eta^8$ -Pn papers was a detailed NMR investigation into the solution phase structure of  $(\eta^8\text{-Pn})\text{Zr}(\text{C}_3\text{H}_5)_2$  by Gabor *et al.*<sup>26</sup> This compound was made in good yield by the combination of  $(\eta^8\text{-Pn})\text{CpZrCl}$  with two equivalents of  $\text{LiC}_3\text{H}_5$ . An NMR investigation elucidated the solution phase structure (implying both allyl units to be bound in an  $\eta^3$  fashion) but geometric details of the complex remained elusive. The Pn\* analogue was therefore targeted, along with the Hf congener, as the ligands' improved crystallizability (compared with Pn)<sup>9,10</sup> could potentially yield the elucidation of geometric parameters.

$[\text{Pn}^*\text{M}(\mu\text{-Cl})_3]_2(\mu\text{-Cl})_2\text{Li}(\text{THF})_x(\text{Et}_2\text{O})_y$  ( $\mathbf{A}_\text{M}$ , M = Zr, Hf)<sup>14</sup> was combined with four equivalents of  $\text{C}_3\text{H}_5\text{MgCl}$  (Scheme 2), after work-up, single crystals of  $\text{Pn}^*\text{M}(\eta^3\text{-C}_3\text{H}_5)_2$  ( $\mathbf{2}_\text{M}$ ) suitable for X-ray diffraction studies were obtained in good yield (59% for  $\mathbf{2}_\text{Zr}$ , 72% for  $\mathbf{2}_\text{Hf}$ ).

### Scheme 2. The synthesis of $\mathbf{2}_\text{M}$ (M = Zr, Hf).



$\mathbf{2}_\text{Zr}$  and  $\mathbf{2}_\text{Hf}$  are isostructural in the solid state, with both crystallizing in the P-1 space group with extremely similar unit cell parameters containing one molecule in the asymmetric unit ( $\mathbf{2}_\text{Zr}$  is shown in Figure 2). Overall the structural metrics are very similar for  $\mathbf{2}_\text{M}$  with slightly shorter M-C bond lengths for  $\mathbf{2}_\text{Hf}$ , which has been previously observed in other  $\text{Pn}^*\text{Hf}$  and  $\text{Pn}^*\text{Zr}$  compounds.<sup>14,16</sup> In the solid state, the allyl units are bound in an  $\eta^3$ -fashion, making  $\mathbf{2}_\text{M}$  18 electron complexes. The allyl units tilt away from the metal centers presumably to optimize the overlap between the d-orbitals on the metals and the p-orbitals of the allyl carbons (demonstrated by the M1-Ct3-C16 and M1-Ct4-C19 angles, Figure 2). The four centroids (two from the Pn\*, one from each of the allyl moieties) arrange themselves as a distorted tetrahedral arrangement around the metal center.

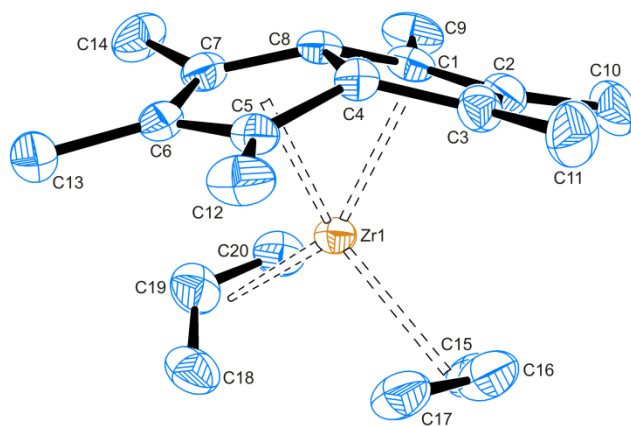


Figure 2: The solid state molecular structure of  $\mathbf{2}_\text{Zr}$ . Thermal Ellipsoids at 50% probability and H-atoms are omitted for clarity. Selected distances (Å) and angles ( $^\circ$ ) for  $\mathbf{2}_\text{Zr}$ : Zr1-Ct1, 2.123(2); Zr1-Ct2, 2.128(2); Zr1-Ct3, 2.270(3); Zr1-Ct4, 2.283(3); Zr1-Ct3-C16 119.6(2); Zr1-Ct4-C19 120.8(3); fold angle 28.5(3). Selected distances (Å) and angles ( $^\circ$ ) for  $\mathbf{2}_\text{Hf}$ : Hf1-Ct1, 2.104(3); Hf1-Ct2, 2.108(3); Hf1-Ct3, 2.245(3); Zr1-Ct4, 2.230(3); Hf1-Ct3-C16, 118.6(2); Hf1-Ct4-C19 117.9(1); fold angle 28.6(4). Ct3 refers to the centroid of C15-C16-C17, Ct4 refers to the centroid of C18-C19-C20.

Due to the previously mentioned thermal instability of group 4 unsubstituted allyl complexes structural comparisons are limited with only one example of a bis  $\eta^3$ -allyl Zr in the literature:  $\text{CpZr}(\eta^3\text{-C}_3\text{H}_5)_2(\eta^1\text{-C}_3\text{H}_5)$ .<sup>27</sup> The structural parameters agree well with this previous example. Even rarer are structurally characterized examples of Hf allyl with only four reported, all containing only one allyl substituent.<sup>28,29</sup> As such  $\mathbf{2}_\text{Hf}$  represents the first structurally characterized bis-allyl Hf compound. The  $\text{Hf-C}_{\text{allyl}}$  distances of  $\mathbf{2}_\text{Hf}$  compare well with the limited examples reported in the CSD.

At room temperature the  $^1\text{H}$  NMR spectrum of  $\mathbf{2}_\text{Hf}$  consists of three resonances, a well-defined quintet at 5.16 ppm ( $J_{\text{H-H}} = 13$  Hz, part of an  $\text{AX}_4$  spin system), a sharp singlet at 1.59 ppm and an extremely broad resonance centered at 1.92 ppm ( $\nu_{1/2} = 91$  Hz; coincident allyl and Pn\* methyl resonances). In contrast the  $\mathbf{2}_\text{Zr}$  spectrum consists of three slightly broadened Pn\* resonances of 6:6:6 intensity ratio ( $\delta = 2.07, 1.71$  and  $1.57$  ppm), whilst the allyl units give five resonances of 2:2:2:2:2 intensity; a multiplet at  $\delta = 5.15$  ppm and four broad doublets at  $\delta = 3.47, 2.45, 1.93$  and  $1.88$  ppm indicating the ligand fluxionality is partially frozen out. Upon cooling of  $\mathbf{2}_\text{Zr}$  and  $\mathbf{2}_\text{Hf}$

their  $^1\text{H}$  NMR spectra can be fully resolved into AMNXY spin systems. Full assignment could be made by inspection of the coupling constants between the terminal allylic protons and the central *meso* proton ( $J_{\text{anti}} = 15\text{ Hz}$ ;  $J_{\text{syn}} = 9\text{ Hz}$ ) in combination with NOESy 2D NMR, whereby the protons of C20/C17 give a cross peak with the protons of the C9/C12 Me groups.

On warming **2<sub>M</sub>** the two NWT-Me proton resonances coalesce to a single resonance concomitant with the CH<sub>2</sub> allyl protons becoming equivalent and the multiplet of the central *meso* proton transforming into a well defined quintet, coupling equally to all the terminal allylic protons (an AX<sub>4</sub> spin system). These NMR data are symptomatic of two possible scrambling mechanisms (Figure 3). Firstly, the allyl ligands can spin at a rate quicker than that of the  $^1\text{H}$  NMR timescale, making the NWT-Me proton equivalent and the two sets of *anti*-/ *syn*- protons equivalent (top scenario of Figure 3). The second scrambling mechanism that could occur is the interchange of the *anti*- and *syn*- protons, which is hypothesized to go via an  $\eta^1:\eta^3$  transition state.<sup>30</sup>

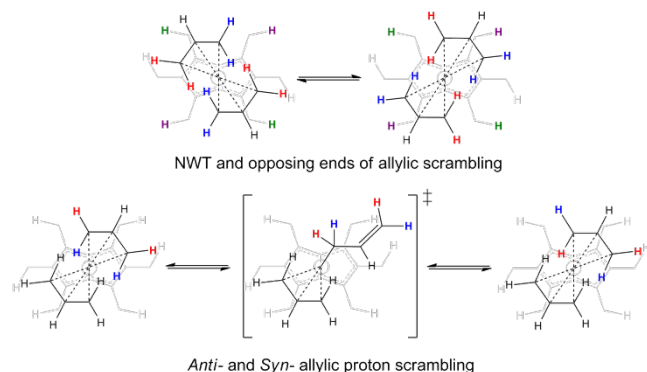
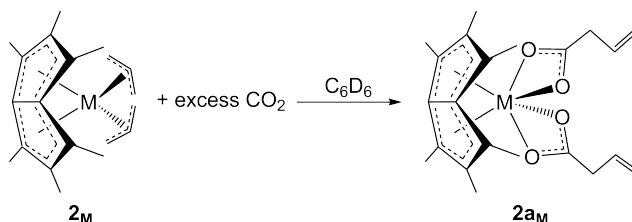


Figure 3: Two possible mechanisms of proton scrambling at work for **2<sub>M</sub>**.

### CO<sub>2</sub> insertion in Pn\*M(allyl)<sub>2</sub> (M = Zr, Hf)

IR spectroscopy of both congeners of **2<sub>M</sub>** revealed a strong signal at 3065 cm<sup>-1</sup> and 1500 cm<sup>-1</sup>, indicative of an  $\eta^1$ -allyl moiety reinforcing the proposed  $\eta^1 \leftrightarrow \eta^3$  intermediate. Should this intermediate be an accurate description of the scrambling mechanism seen, it was proposed that addition of CO<sub>2</sub> may result in insertion of the molecule into the M-C  $\sigma$ -bond and trapping out of this intermediate.<sup>17</sup> An NMR sample of **2<sub>M</sub>** (M = Zr, Hf) was charged with CO<sub>2</sub> this resulted in a swift lightening in color of the solution. The resulting  $^1\text{H}$  NMR spectrum consisted of seven resonances; three sharp singlets in the region expected for Pn\* Me groups (integral ratio 6:6:6), a doublet positioned around  $\delta = 3\text{ ppm}$  (corresponding to the  $sp^3$  hybridized CH<sub>2</sub> group, integral ratio 2), two overlapping doublet of multiplets at approximately  $\delta = 5\text{ ppm}$  (overall integral ratio 4) and a multiplet at just below  $\delta = 6\text{ ppm}$  (integral ratio 2). These data are consistent with the proposed CO<sub>2</sub> inserted species Pn\*M( $\kappa^2$ -O<sub>2</sub>CCH<sub>2</sub>CHCH<sub>2</sub>)<sub>2</sub> (**2a<sub>M</sub>**, Scheme 2). The  $^{13}\text{C}$  NMR data also showed the expected low field resonance for the  $\kappa^2$ -O<sub>2</sub>CR ( $\delta = 191\text{ ppm}$ ). All this data suggests the bottom scrambling scenario of Figure 3 is occurring.



Scheme 3. The double insertion of CO<sub>2</sub> in the M-allyl groups in **2<sub>M</sub>** (M = Zr, Hf).

The  $\eta^1 \leftrightarrow \eta^3$  allyl conversion would not however cause the two NWT-Me environments to coalesce, so the top scenario of Figure 3 must also be occurring. By inspection of the line shape at the point of coalescence in the  $^1\text{H}$  NMR spectrum, it is possible to calculate the energy barrier for this scrambling mechanism. This was found to be 63.4 kJ mol<sup>-1</sup> for **2<sub>Zr</sub>** and 58.4 kJ mol<sup>-1</sup> for **2<sub>Hf</sub>** (at 43 °C and 15 °C respectively). These values are both comparable with that found for PnZr(C<sub>3</sub>H<sub>5</sub>)<sub>2</sub> (64.0 kJ mol<sup>-1</sup>).<sup>26</sup>

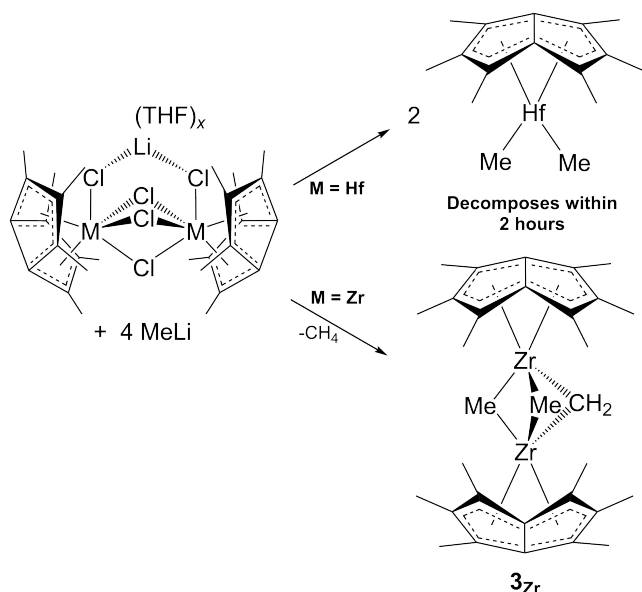
**2<sub>Hf</sub>** and **2<sub>Zr</sub>** were also characterized by high resolution mass spectrometry showing signals at the relevant molecular ion peak ( $m/z = 358.1232$  for **2<sub>Zr</sub>** and 448.1652 for **2<sub>Hf</sub>**) and the subsequent fragmentation pattern of loss of the allylic groups and then the breakdown of the Pn\* ring.

### Synthesis of “Pn\*M(methyl)” (M = Zr, Hf) complexes

Addition of four equivalents of MeLi to **A<sub>Zr</sub>** resulted in the solution changing from golden yellow in color to a ruby red hue. Subsequent work-up yielded a red microcrystalline solid in good yield (64%).  $^1\text{H}$  NMR studies demonstrated there to be two different non-Pn\* proton environments, and subsequent single crystal X-ray diffraction analysis revealed the structure to comprise of a “Pn\*Zr” dimer bridged by three groups, two methyl and one methylene unit: (Pn\*Zr)<sub>2</sub>( $\mu$ -CH<sub>2</sub>)( $\mu$ -Me)<sub>2</sub> (**3<sub>Zr</sub>**). To date it has not been possible to synthesize the Hf derivative of **3<sub>Zr</sub>**. A parallel synthesis results in the formation of an orange solution, which exhibits three signals in the  $^1\text{H}$  NMR spectrum in a 12:6:6 intensity ratio. This compound was found to be thermally unstable, decomposing when heated or left at room temperature overnight, either in solution or in the solid state, giving methane gas and an unidentified extremely pyrophoric yellow solid.

We postulate that on addition of MeLi the dimer [Pn\*MMe( $\mu$ -Cl)]<sub>2</sub> is initially formed. In the case of Zr, methane is quickly eliminated to give (Pn\*Zr)<sub>2</sub>( $\mu$ -CH<sub>2</sub>)( $\mu$ -Cl)<sub>2</sub>, which subsequently undergoes metathesis with two further equivalents of MeLi to form the 16 e<sup>-</sup> complex **3<sub>Zr</sub>**. For the Hf congener it is thought that the second metathesis occurs at a quicker rate than elimination of methane, thus forming the species Pn\*HfMe<sub>2</sub> (Scheme 4), which is unstable to decomposition to unknown organometallic products and methane.





**Scheme 4.** The synthesis of  $3_{Zr}$ , and the proposed alternate reaction for  $3_{Hf}$ .

Single crystals of  $3_{Zr}$  were grown from the slow evaporation of a saturated toluene solution, under an inert atmosphere.  $3_{Zr}$  crystallizes in the  $P2_1$  space group in two molecules with the asymmetric unit. One molecule is shown in Figure 4 (the other is comparable).

It was not possible to directly locate the hydrogens on the electron density map, however, inspection of bond lengths reveals one carbon (C16) to have a considerably shorter average Zr-C distance, and is therefore proposed to be the  $\mu$ -CH<sub>2</sub> group. The stronger interaction of the formally CH<sub>2</sub><sup>2-</sup> group with the two metal centers results in a pinching of the two 'Pn\*Zr' fragments thus preventing them from being parallel.

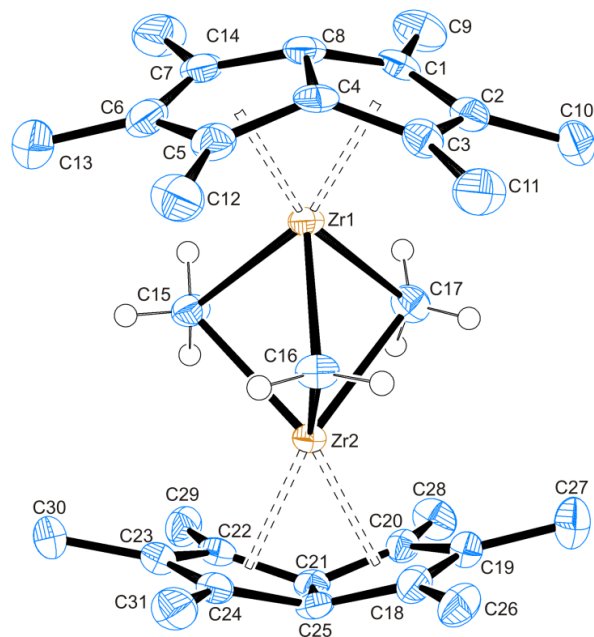


**Figure 4:** The solid state molecular structure of  $3_{Zr}$ . Thermal ellipsoids at 50% probability, H-atoms of the Pn\* rings omitted for clarity. Selected distances (Å) and angles (°) for  $3_{Zr}$ : Zr1-Ct1, 2.097(2); Zr1-Ct2, 2.111(3); Zr1-C15, 2.436(5); Zr1-C16

2.278(5), Zr1-C17 2.473(6); Zr1-Zr2 3.052(1); Zr2-Ct3, 2.114(3); Zr2-Ct4 2.111(3); Zr2-C15, 2.447(6), Zr2-C16, 2.257(5); Zr2-C17, 2.445(6); fold angles, 30.3(5), 31.2(5); tilt angle, 29.5°. Ct3 is the centroid of ring C18-C19-C20-C21-C25, Ct4 is the centroid of C21-C22-C23-C24-C25; tilt angle is defined as the angle between the Ct1-Zr1-Ct2 plane and the Ct3-Zr2-Ct4 plane.

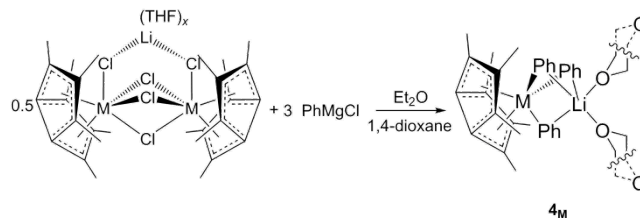
The Zr centers adopt an approximately square based pyramidal arrangement, with the two  $\mu$ -Me groups and the Pn\*<sub>cent.</sub> forming the base. The fold angle and M-Pn\* distances of  $3_{Zr}$  are comparable to the previously reported Pn\*ZrCp derivatives.<sup>16</sup>

Crystallographically characterized  $\mu$ -Me and  $\mu$ -CH<sub>2</sub> moieties located between two Zr centers are relatively rare.<sup>31–40</sup>  $3_{Zr}$  is the first structurally characterized example of a bimetallic system involving three  $\mu$ -Me/CH<sub>2</sub> groups. The average Zr-( $\mu$ -CH<sub>2</sub>) distance (2.268 Å) is slightly longer than examples found in the CSD. For instance [(ZrCpMe)<sub>2</sub>( $\mu$ -CH<sub>2</sub>)<sub>2</sub>][B(C<sub>6</sub>F<sub>5</sub>)<sub>4</sub>]<sup>−</sup> has an average distance of 2.234 Å, and for [ZrCp\*(C<sub>2</sub>B<sub>9</sub>H<sub>11</sub>)<sub>2</sub>]( $\mu$ -CH<sub>2</sub>) the average distance is 2.182 Å.<sup>31,34</sup> The average Zr-( $\mu$ -Me) distance (2.448 Å) is comparable to literature examples, even for those systems which are cationic.<sup>39</sup>

The room temperature <sup>1</sup>H NMR spectrum of  $3_{Zr}$  consists of four resonances of integral ratio 2:24:12:6 at  $\delta$  = 2.71, 1.96, 1.92 and −0.38 ppm respectively. On cooling  $3_{Zr}$ , no evidence was seen of any decoalescence phenomenon and it can therefore be assumed that the Pn\* rings are quickly rotating about the metal/bridgehead centroid axis. The methylene resonance comes somewhat upfield of other documented examples, showing it to be relatively more shielded.<sup>31,41</sup> The <sup>13</sup>C{<sup>1</sup>H} NMR of  $3_{Zr}$  shows five expected Pn\* resonances and two further resonances at  $\delta$  = 38.9 and 127.9 ppm [corresponding to the ( $\mu$ -Me) and ( $\mu$ -CH<sub>2</sub>) resonances respectively]. Similar to the <sup>1</sup>H NMR spectrum the methylene <sup>13</sup>C NMR resonance is shifted considerably upfield, however the coupling constant seen in the decoupled spectrum is typical of a bridging methylene (<sup>1</sup>J<sub>C-H</sub> = 115.4 Hz). The attempted Hf reaction gave a <sup>1</sup>H NMR spectrum consisting of three resonances at  $\delta$  = 2.10, 1.96 and −0.44 ppm, in a 12:6:6 integral ratio. The furthest upfield shift is typical for terminal Hf-Me groups (e.g. Cp\*HfMe<sub>2</sub>  $\delta_{Me}$  = 0.07 ppm) and therefore the formulation depicted in Scheme 4 is proposed.<sup>42</sup>

#### Synthesis of [Pn\*M(Ph)<sub>3</sub>]<sup>−</sup> (M = Zr, Hf)

[Pn\*M(Ph)<sub>3</sub>]<sup>−</sup> (M = Zr, Hf) were synthesized by rapid addition of PhMgBr (3.0 M in Et<sub>2</sub>O) to **A<sub>M</sub>**, followed by addition of 1,4-dioxane in order to precipitate the magnesium salts.<sup>43</sup> <sup>1</sup>H NMR integral analysis revealed the 'Pn\*M' fragment had been triply arylated and therefore an initial formulation of Pn\*MPh<sub>3</sub>·Li was proposed. However structural elucidation revealed that 1,4-dioxane had been incorporated into the structure to give a polymeric structure with bridging 1,4-dioxane; [Pn\*ZrPh(μ-Ph)<sub>2</sub>Li(μ-1,4-dioxane)]<sub>n</sub> (**4<sub>Zr</sub>**, Scheme 5). To date it has not been possible to grow single crystals of **4<sub>Hf</sub>**.



**Scheme 5.** The synthesis of  $4_M$  (M = Zr, Hf).

Single crystals of  $\mathbf{4}_{\text{Zr}}$  suitable for X-ray diffraction were grown from a saturated hexane solution slow cooled to  $-38\text{ }^{\circ}\text{C}$ .  $\mathbf{4}_{\text{Zr}}$  crystallizes in the  $P-1$  space group with a single molecule in the asymmetric unit of the unit cell. A diagram of a monomer unit is shown in Figure 5(A) and reveals the metal center to be surrounded by three Ph groups with a lithium cation bound to two of them (through the *ipso* carbon) in order to charge balance. Presumably  $\mathbf{4}_{\text{Zr}}$  binds three Ph moieties in order to minimize its coordinative and electronic unsaturation (binding two phenyl  $\text{Pn}^*\text{MPh}_2$  would be a  $14\text{ e}^-$  complex, whereas  $\mathbf{4}_{\text{M}}$  may be viewed as an  $16\text{ e}^-$  complex). This has already been seen in the dimerization of the starting material  $\mathbf{A}_{\text{M}}$  and its incorporation of  $\text{LiCl}$ .<sup>14</sup> The Li is solvated by two molecules of 1,4-dioxane which bridge to another lithium cation in an adjacent monomer unit and thus form a 1-dimensional polymer extending in the *ab*-plane [Figure 5(B)].

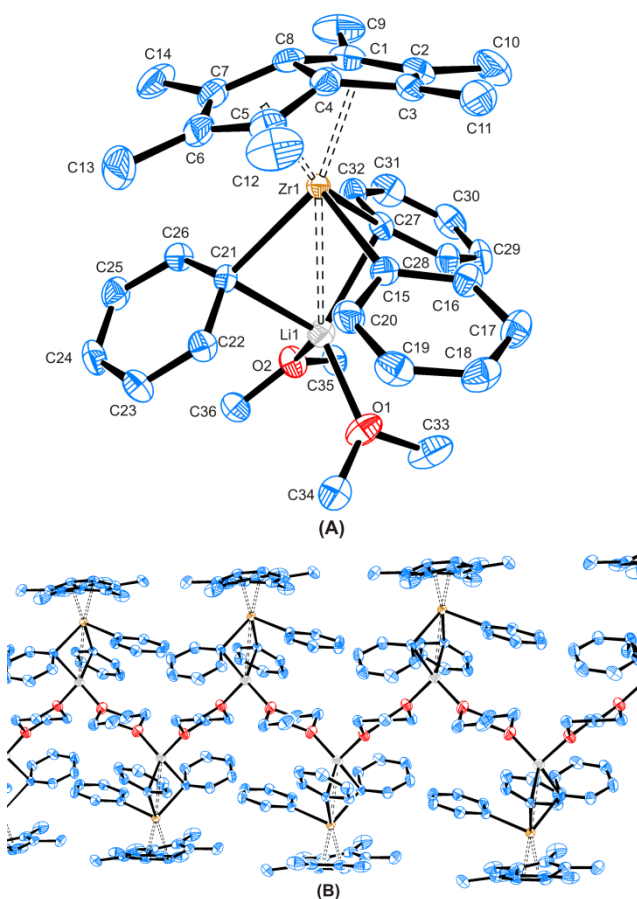


Figure 5: (A) The solid state molecular structure of an asymmetric unit of  $\mathbf{4}_{\text{Zr}}$ , (B) The polymeric structure of  $\mathbf{4}_{\text{Zr}}$  viewed with respect to the *ab*-plane (the *ab*-plane is the plane of the page). Thermal ellipsoids at 50% probability and H-atoms omitted for clarity. Selected distances ( $\text{\AA}$ ) and angles ( $^{\circ}$ ) for  $\mathbf{4}_{\text{Zr}}$ : Zr1-Ct1, 2.154(2); Zr1-Ct2, 2.148(2); Zr1-C15, 2.336(2); Zr1-C21, 2.404(2); Zr1-C27, 2.403(2); Zr1-Li1, 3.172(3); Li1-C21, 2.282(4); Li1-C27, 2.290(4), fold angle:  $27.9(2)$ .

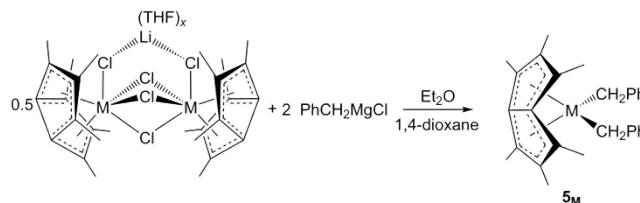
Documented Zr-Ph compounds are common however, only one is known in combination with a coordinated lithium cation.<sup>44</sup> In this example there are two different Zr-Ph distances [ $2.367(4)$  and  $2.450(4)\text{ \AA}$ ], due to the former phenyl being bound to a single lithium and the latter bound to two Li cations. The average Zr-( $\mu$ -Ph) distance in  $\mathbf{4}_{\text{Zr}}$  is  $2.403(2)$ , similar to the previous example despite the presence of only one Li. The Zr-C(15) distance in  $\mathbf{4}_{\text{Zr}}$  is slightly longer than those found

for  $\text{ZrCp}^*_2\text{Ph}_2$  ( $2.311\text{ \AA}$ ) and  $\text{ZrCp}_2\text{Ph}_2$  ( $2.301\text{ \AA}$ ).<sup>45,46</sup> Since these examples are formally  $16\text{ e}^-$  complexes, the slight lengthening in  $\mathbf{4}_{\text{Zr}}$  can be attributed to increased steric crowding around the Zr center. The  $\text{Pn}^*$  ligand in  $\mathbf{4}_{\text{Zr}}$  is considerably flatter and has longer M-Pn\*<sub>cent.</sub> distances than  $\mathbf{3}_{\text{Zr}}$  (fold angles:  $27.9(2)^{\circ}$  for  $\mathbf{4}_{\text{Zr}}$ , average  $30.6(5)^{\circ}$  for  $\mathbf{3}_{\text{Zr}}$ ; M-Pn\*<sub>cent.</sub> average:  $2.151(3)\text{ \AA}$  for  $\mathbf{4}_{\text{Zr}}$ ;  $2.109(4)$  for  $\mathbf{3}_{\text{Zr}}$ ). This is due to the greater steric demand of the phenyl ligands compared the methyl and methylene ligands.

The  $^1\text{H}$  NMR spectra of  $\mathbf{4}_{\text{M}}$  consist of six resonances of 6:6:3:8:12:6 integral ratio (corresponding to the three phenyl, dioxane and the two  $\text{Pn}^*$  methyl environments). Due to the similarity of  $\mathbf{4}_{\text{Hf}}$  to  $\mathbf{4}_{\text{Zr}}$  spectra, and the persistence of 1,4-dioxane within the product, it is proposed  $\mathbf{4}_{\text{Hf}}$  is isostructural with  $\mathbf{4}_{\text{Zr}}$ . The presence of a three unique  $^1\text{H}$  resonances for the Ph ligands implies all three ligands are equivalent on the NMR timescale and the lithium is either undergoing a fluxional process to bind to each Ph or is not bound in the solution phase. The 1,4-dioxane cannot be removed. The  $^{13}\text{C}\{^1\text{H}\}$  NMR spectrum shows the presence of ten expected resonances and the  $^7\text{Li}$  NMR shows a sharp singlet ( $\delta = -1.12$  and  $-1.06\text{ ppm}$  for  $\mathbf{4}_{\text{Zr}}$  and  $\mathbf{4}_{\text{Hf}}$  respectively).

#### Synthesis of $\text{Pn}^*\text{M}(\text{CH}_2\text{Ph})_n$ ( $\text{M} = \text{Zr}, \text{Hf}$ ) complexes

Addition of four equivalents of  $\text{PhCH}_2\text{MgCl}$  to  $\mathbf{A}_{\text{M}}$  and subsequent work-up results in the formation of  $\mathbf{5}_{\text{M}}$  ( $\text{M} = \text{Zr}, \text{Hf}$ ) (Scheme 6).



Scheme 6. The synthesis of  $[(\text{Pn}^*)\text{Zr}(\text{CH}_2\text{Ph})_2]$ ;  $\mathbf{5}_{\text{Zr}}$ .

A saturated hexane solution of  $\mathbf{5}_{\text{Zr}}$  was slow cooled to  $-38\text{ }^{\circ}\text{C}$  over three days, resulting in the precipitation of a fine powder. The supernatant was removed *via* filter cannula, concentrated and then again cooled to  $-38\text{ }^{\circ}\text{C}$ . This process was repeated once more to yield red crystals of  $\mathbf{5}_{\text{Zr}}$  suitable for X-ray analysis (in 53% yield).  $\mathbf{5}_{\text{Zr}}$  crystallizes in the  $P2_1/n$  space group with a single molecule in the asymmetric unit of the unit cell. In contrast to  $\mathbf{3}_{\text{Zr}}$  and  $\mathbf{4}_{\text{Zr}}$ ,  $\mathbf{5}_{\text{Zr}}$  exists as a monomeric complex as shown in Figure 6. The Zr centers adopt an approximately tetrahedral arrangement.

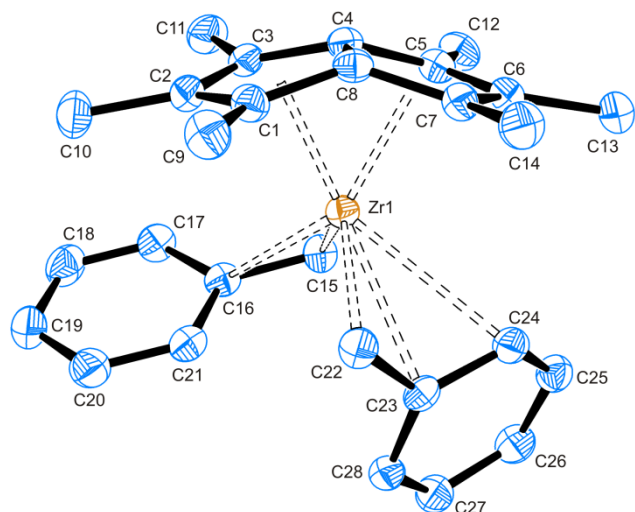
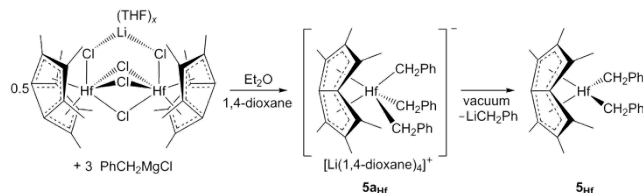


Figure 6: The solid state molecular structure of **5<sub>Zr</sub>**. Thermal ellipsoids at 50% probability and H-atoms omitted for clarity. Selected distances (Å) and angles (°) for **5<sub>Zr</sub>**: Zr1-Ct1, 2.094(2); Zr1-Ct2, 2.122(2); Zr1-C15, 2.323(4); Zr1-C16, 2.862(3); Zr1-C21, 3.005(3); Zr1-C22, 2.378(3); Zr1-C23, 2.666(3); Zr1-C24, 2.858(3); Zr1-C25, 3.800(3); Zr1-C15-C16, 95.5(2); Zr1-C22-C23, 84.2(2); fold angle, 28.8(3).

The benzyl ligand is known to bind to transition metal centers in a variety of coordination modes (ranging from  $\eta^1$  to  $\eta^7$ ) depending on the electron deficient nature of the metal. Strict assignment of the hapticity was often a fairly subjective issue until Parkin *et al.* undertook an in-depth investigation into bonding in Zr-benzyl species.<sup>47</sup> This study revealed two ways of distinguishing the bonding mode of a benzyl ligand, firstly the deviation of the M-CH<sub>2</sub>-Ph bond angle from the idealized 109.5° (which can identify between  $\eta^1$  and higher hapticities), and secondly the difference between the M-CH<sub>2</sub> and M-C<sub>Ph</sub> distances (which can differentiate between the higher hapticities). To this end Parkin and coworkers introduce the  $\delta$  value (defined in Figure S1, see supporting information). Using these two values Parkin was able to propose definitive assignment of binding modes of benzyl complexes (summarized in Table S1). The  $\delta$  values for **5<sub>Zr</sub>** are in Table S2 (see supplementary information) predict hapticities of  $\eta^3$  for one benzyl and the other lies between the  $\eta^1$  and  $\eta^2$  definitions. The former prediction is supported by DFT analysis (Figure S2). Inspection of the molecular orbitals shows only one bonding interaction in the lowest energy of the valence orbitals (HOMO-9, figure S3) and as such an  $\eta^1$  bonding motif is tentatively assigned.

There is a significant difference in Zr-Pn\*<sub>cent.</sub> distances within **5<sub>Zr</sub>**, which is ascribed to the different binding modes of the two benzyl units. The  $\eta^3$  benzyl must align the p-orbital of the near-side ortho carbon (C24) with the d-orbitals of the metal center, this results in a steric clash with the Pn\* wing tip(WT)-Me and NWT-Me (C13/C14) thus forcing up this side of the Pn\* and leading to a large Zr-Pn\*<sub>cent.</sub> distance. The other benzyl does not require such orbital overlap and is therefore able to angle the aromatic ring away from the Pn\* ligand resulting in less of a steric clash. The Pn\* fold angle of 28.8(3)°, lies between **3<sub>Zr</sub>** and **4<sub>Zr</sub>** [average of 30.7(5)° and 27.9(2)° respectively]. This can be attributed to steric considerations, with the tri-substituted **4<sub>Zr</sub>** being more sterically encumbered than **5<sub>Zr</sub>**, with both having greater steric bulk than **3<sub>Zr</sub>**.

Unfortunately crystals of **5<sub>Hf</sub>** suitable for single crystal X-ray analysis could not be obtained, however following addition to 1,4-dioxane during work-up yellow crystals of an intermediate were formed and identified as [Pn\*Hf(CH<sub>2</sub>Ph)<sub>3</sub>]<sup>+</sup>[Li(1,4-dioxane)<sub>4</sub>]<sup>-</sup> (**5a<sub>Hf</sub>**, scheme 7). **5a<sub>Hf</sub>** crystallized in the Cc space group with a single molecule in the asymmetric unit of the unit cell. This species consists of a triply benzylated 'Pn\*Hf' anionic fragment and a lithium counter-ion coordinated by four 1,4-dioxane molecules. Unlike **4<sub>Zr</sub>**, there appears to be no covalent interaction between the anion and cation within the solid state structure and upon exposure to vacuum the 1,4-dioxane was removed, subsequently precipitating LiCH<sub>2</sub>Ph and forming **5<sub>Hf</sub>** (demonstrated by <sup>1</sup>H NMR and <sup>7</sup>Li NMR spectroscopy). A model of the anion of **5a<sub>Hf</sub>** is shown in Figure 7.



Scheme 7: The synthesis of [Pn\*Hf(CH<sub>2</sub>Ph)<sub>3</sub>][Li(1,4-dioxane)<sub>4</sub>], **5a<sub>Hf</sub>**.

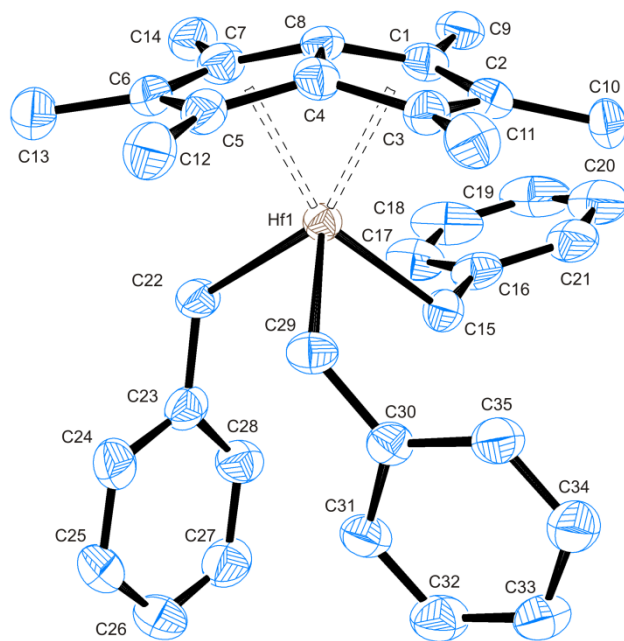


Figure 7: The solid state molecular structure of **5a<sub>Hf</sub>**. Thermal ellipsoids at 50% probability, H-atoms and counter ion [Li(1,4-dioxane)<sub>4</sub>]<sup>+</sup> omitted for clarity. Selected distances (Å) and angles (°) for **5a<sub>Hf</sub>**: Hf1-Ct1, 2.164(3); Hf1-Ct2, 2.180(3); Hf1-C15, 2.316(5); Hf1-C16, 3.326(7); Hf1-C22, 2.322(5); Hf1-C23, 3.258(6); Hf1-C29, 2.342(5); Hf1-C30, 3.377(5); Hf1-C15-C16, 121.2(4); Hf1-C22-C23, 116.5(4); Hf1-C29-C30, 123.0(4); fold angle, 24.5(6).

The geometry about the Hf center is approximately square-pyramidal with the two Pn\*<sub>cent.</sub> C(22) and C(15) making up the square base. Of the three benzyl ligands, two are aligned perpendicular to the Pn\* ligand [C(22)-C(28) and C(29)-C(35)] and one is lying parallel to it [C(15)-C(21)], which appears to be the result of crystal packing forces. It is clear by inspection of the Hf-CH<sub>2</sub>-Ph bond angles that all three ligands are bound in an  $\eta^1$ -fashion, something that is also confirmed by extending Parkin's  $\delta$  parameter to Hf (all of which are over 0.5 Å).

The Hf-C(15/22/29) bond lengths are all comparable to Zr-C(15) in **5<sub>Zr</sub>**. The Hf-CH<sub>2</sub> distances are also comparable to those in the related benzyl compounds, HfCp<sub>2</sub>(CH<sub>2</sub>Ph)<sub>2</sub> [average = 2.29(1) Å]<sup>48</sup> and HfCp\*(CH<sub>2</sub>Ph)<sub>3</sub> [average = 2.26(3) Å].<sup>49</sup>

The Pn\* ligand of **5<sub>Hf</sub>** has a considerably increased M-Pn\*<sub>cent.</sub> Distance compared to **5<sub>Zr</sub>** (2.169 Å and 2.108 Å respectively) as well as a relative flattening of the ligand [fold angles 24.7(6)° and 28.8(3)° respectively]. This difference is attributed both to electronic factors, with **5<sub>Hf</sub>** being an anionic complex, it would be expected that the (formally anionic) ligands would be more distant to the metal center in order to minimize repulsion, and also due to steric considerations, with **5<sub>Hf</sub>** having three benzyl groups in the metal coordination sphere compared to two for **5<sub>Zr</sub>**.

Following work-up and subjection to vacuum, **5<sub>Hf</sub>** transforms to be structurally analogous with **5<sub>Zr</sub>** (from careful inspection of the integrals in the <sup>1</sup>H NMR spectrum). Both congeners of **5<sub>M</sub>** exhibit C<sub>2v</sub> symmetry in solution, with six resonances in the <sup>1</sup>H NMR spectrum of 4:2:4:12:6:4 integral ratio. The three furthest downfield lying in the aromatic region (δ = 6–7 ppm), and the remainder lying upfield in the aliphatic region (δ = 1–2 ppm). The <sup>13</sup>C NMR spectra of **5<sub>M</sub>** exhibit 10 resonances, five for Pn\* and five for the benzyl ligands. Latesky and co-workers noted that the coupling constant of the α-CH<sub>2</sub> group and the chemical shift of the ortho protons could be used to probe the binding situation of benzyl ligands, the corresponding data for compounds **5<sub>M</sub>** (M = Zr and Hf) are summarized in Table 2.<sup>50</sup> In cases where there is significant π interaction between the benzyl ligand and the metal center the chemical shift of the *ortho* protons migrates upfield and the <sup>1</sup>J<sub>C-H</sub> increases relative to those observed for the other benzyl carbons. Both these effects are clearly seen for **5<sub>Zr</sub>**, where δ = 6.06 ppm and <sup>1</sup>J<sub>C-H</sub> = 135 Hz and as such the proposed η<sup>3</sup>:η<sup>1</sup> binding modes are reinforced. Comparatively Latesky's analysis for **5<sub>Hf</sub>** implies the benzyl ligands to be bound with more η<sup>1</sup> character than **5<sub>Zr</sub>**. However, there is a slight increase in the <sup>1</sup>J<sub>C-H</sub> coupling parameter and the *ortho* chemical shift is slightly upfield compared with species where the benzyl is bound in an explicitly η<sup>1</sup> fashion, therefore it is likely the binding mode lies somewhere in between the η<sup>1</sup> and η<sup>2</sup> modes.

**Table 2. The <sup>1</sup>H and <sup>13</sup>C NMR chemical shifts of the phenyl ortho nuclei and the <sup>1</sup>J<sub>C-H</sub> of the CH<sub>2</sub> group of **5<sub>M</sub>** (M = Zr, Hf)**

Species	<sup>1</sup> H δ (ppm)	<sup>13</sup> C δ (ppm)	CH <sub>2</sub> <sup>1</sup> J <sub>C-H</sub> (Hz)
<b>5<sub>Zr</sub></b>	6.06	122.5	135.0
<b>5<sub>Hf</sub></b>	6.50	124.0	129.0

## CONCLUSION

A series of group 4 permethylpentadiene “Pn\*M” compounds have been synthesized. Pn\*<sub>2</sub>M (M = Zr, Hf) present a pair of highly sterically encumbered compounds, that do not show disorder in the solid state like their f-block analogues. The rare group 4 bis(allyl) species, Pn\*M(C<sub>3</sub>H<sub>5</sub>)<sub>2</sub> (M = Zr, Hf) were observed to be fluxional in solution and spontaneously react with CO<sub>2</sub> to give the double insertion product Pn\*M(κ<sup>2</sup>-O<sub>2</sub>CCH<sub>2</sub>CHCH<sub>2</sub>)<sub>2</sub> (M = Zr, Hf). A series of “Pn\*M” (M = Zr and Hf) derivatives containing hydrocarbyl ligands has been isolated. Of particular note is (Pn\*Zr)<sub>2</sub>(μ-CH<sub>2</sub>)(μ-Me)<sub>2</sub>, which has a unique structural motif containing 3 (μ-CH<sub>2</sub>) and/or (μ-

Me) moieties. Further, the benzyl complexes [Pn\*M(CH<sub>2</sub>Ph)<sub>n</sub>]<sup>0/-1</sup> (M = Zr and Hf) display characteristic benzyl ligation ranging from η<sup>1</sup>:η<sup>3</sup> to η<sup>2</sup>:η<sup>2</sup> bonding of the benzyl ligands.

## ASSOCIATED CONTENT

### Supporting Information

Supporting information is available free of charge on the ACS Publications website at DOI: 10.1021/acs.organomet....

Crystal data and full experimental details and characterizing data for **1<sub>M</sub>**–**5<sub>M</sub>** (PDF)

X-ray crystallographic data for compounds **1<sub>Zr</sub>**, **1<sub>Hf</sub>**, **2<sub>Zr</sub>**, **3<sub>Zr</sub>**, **4<sub>Zr</sub>**, **5<sub>Zr</sub>**, **5<sub>Hf</sub>** (CIF).

## AUTHOR INFORMATION

### Corresponding Author

\* E-mail: dermat.ohare@chem.ox.ac.uk

### Author Contributions

The manuscript was written through contributions of all authors.

### Notes

The authors declare no competing financial interest.

## ACKNOWLEDGMENT

The authors would like to thank the Engineering and Physical Sciences Research Council (EPSRC) for financial support via grants EP/P505216/1 and EP/P503876/1.

## REFERENCES

- (1) King, R. B. *Appl. Organomet. Chem.* **2003**, *17* (6–7), 393–397.
- (2) Katz, T. J. *J. Am. Chem. Soc.* **1960**, *82* (14), 3784–3785.
- (3) Katz, T. J.; Rosenberger, M. *J. Am. Chem. Soc.* **1962**, *84* (5), 865–866.
- (4) Green, J. C.; Green, M. L. H.; Parkin, G. *Chem. Commun.* **2012**, 11481–11503.
- (5) Abbasali, Q. A.; Cloke, F. G. N.; Hitchcock, P. B.; Joseph, S. C. P. *Chem. Commun.* **1997**, 1541–1542.
- (6) Cloke, F. G. N.; Hitchcock, P. B.; Kuchta, M. C.; Morley-Smith, N. A. *Polyhedron* **2004**, *23* (17), 2625–2630.
- (7) Jonas, K.; Kolb, P.; Kollbach, G.; Gabor, B.; Mynott, R.; Angermund, K.; Heinemann, O.; Krüger, C. *Angew. Chemie Int. Ed.* **1997**, *36* (16), 1714–1718.
- (8) Summerscales, O. T.; Cloke, F. G. N. *Coord. Chem. Rev.* **2006**, *250* (9–10), 1122–1140.



- (9) Ashley, A. E.; Cowley, A. R.; O'Hare, D. *Chem. Commun.* **2007**, 1512–1514.
- (10) Ashley, A. E.; Cowley, R. A.; O'Hare, D. *European J. Org. Chem.* **2007**, 14, 2239–2242.
- (11) Ashley, A.; Balazs, G.; Cowley, A.; Green, J.; Booth, C. H.; O'Hare, D. *Chem. Commun.* **2007**, 1515–1517.
- (12) Chadwick, F. M.; Ashley, A.; Wildgoose, G.; Goicoechea, J. M.; Randall, S.; O'Hare, D. *Dalton Trans.* **2010**, 39 (29), 6789–6793.
- (13) Chadwick, F. M.; O'Hare, D. M. *Organometallics* **2014**, 33 (14), 3768–3774.
- (14) Cooper, R. T.; Chadwick, F. M.; Ashley, A. E.; O'Hare, D. *Organometallics* **2013**, 32 (7), 2228–2233.
- (15) Kilpatrick, A. F. R.; Cloke, F. G. N. *Chem. Commun.* **2014**, 2769–2771.
- (16) Chadwick, F. M.; Cooper, R. T.; Ashley, A. E.; Buffet, J.-C.; O'Hare, D. M. *Organometallics* **2014**, 33 (14), 3775–3785.
- (17) Cooper, R. T.; Chadwick, F. M.; Ashley, A. E.; O'Hare, D. *Chem. Commun.* **2015**, 11856–11859.
- (18) Gleiter, R.; Bethke, S.; Okubo, J.; Jonas, K. *Organometallics* **2001**, 20 (20), 4274–4278.
- (19) Bendjaballah, S.; Kahlal, S.; Costuas, K.; Bévilion, E.; Saillard, J.-Y. *Chemistry* **2006**, 12 (7), 2048–2065.
- (20) Li, H.; Feng, H.; Sun, W.; Xie, Y.; King, R. B.; Schaefer III, H. F. *New J. Chem.* **2011**, 35 (8), 1718.
- (21) Ashley, A. E.; Cooper, R. T.; Wildgoose, G. G.; Green, J. C.; O'Hare, D. *J. Am. Chem. Soc.* **2008**, 130 (46), 15662–15677.
- (22) Wilke, G.; Bogdanović, B.; Hardt, P.; Heimbach, P.; Keim, W.; Kröner, M.; Oberkirch, W.; Tanaka, K.; Steinrücke, E.; Walter, D.; Zimmermann, H. *Angew. Chemie Int. Ed.* **1966**, 5 (2), 151–164.
- (23) Ballard, D. G. H. *Adv. Catal.* **1973**, 23, 263–325.
- (24) Solomon, S. A.; Layfield, R. A. *Dalton Trans.* **2010**, 39 (10), 2469–2483.
- (25) Martin, H. A.; Lemaire, P. J.; Jellinek, F. *J. Organomet. Chem.* **1968**, 14 (1), 149–156.
- (26) Gabor, B.; Jonas, K.; Mynott, R. *Inorganica Chim. Acta* **1998**, 270 (1–2), 555–558.
- (27) Erker, G.; Berg, K.; Angermund, K.; Krueger, C. *Organometallics* **1987**, 6 (12), 2620–2621.
- (28) Pindado, G. J.; Thornton-Pett, M.; Bochmann, M. *J. Chem. Soc. Dalton Trans.* **1997**, 18, 3115–3128.
- (29) Pastor, A.; Kiely, A. F.; Henling, L. M.; Day, M. W.; Bercaw, J. E. *J. Organomet. Chem.* **1997**, 528 (1–2), 65–75.
- (30) Highcock, W. J.; Mills, R. M.; Spencer, J. L.; Woodward, P. *J. Chem. Soc. Dalton Trans.* **1986**, 4, 829.
- (31) Hogenbirk, M.; Schat, G.; Akkerman, O. S.; Bickelhaupt, F.; Schottek, J.; Albrecht, M.; Fröhlich, R.; Kehr, G.; Erker, G.; Kooijman, H.; Spek, A. L. *Eur. J. Inorg. Chem.* **2004**, 2004 (6), 1175–1182.
- (32) Waymouth, R. M.; Santarsiero, B. D.; Grubbs, R. H. *J. Am. Chem. Soc.* **1984**, 106 (14), 4050–4051.
- (33) Wilson, P. A.; Wright, J. A.; Oganessian, V. S.; Lancaster, S. J.; Bochmann, M. *Organometallics* **2008**, 27 (23), 6371–6374.
- (34) Crowther, D. J.; Baenziger, N. C.; Jordan, R. F. *J. Am. Chem. Soc.* **1991**, 113 (4), 1455–1457.
- (35) Duncan, A. P.; Mullins, S. M.; Arnold, J.; Bergman, R. G. *Organometallics* **2001**, 20 (9), 1808–1819.
- (36) Chen, Y.-X.; Stern, C. L.; Yang, S.; Marks, T. J. *J. Am. Chem. Soc.* **1996**, 118 (49), 12451–12452.
- (37) Buchwald, S. L.; Lucas, E. A.; Davis, W. M. *J. Am. Chem. Soc.* **1989**, 111 (1), 397–398.
- (38) Waymouth, R. W.; Potter, K. S.; Schaefer, W. P.; Grubbs, R. H. *Organometallics* **1990**, 9 (10), 2843–2846.
- (39) Keaton, R. J.; Jayaratne, K. C.; Fetting, J. C.; Sita, L. R. *J. Am. Chem. Soc.* **2000**, 122 (51), 12909–12910.
- (40) Wang, C.; van Meurs, M.; Stubbs, L. P.; Tay, B.-Y.; Tan, X.-J.; Aitipamula, S.; Chacko, J.; Luo, H.-K.; Wong, P.-K.; Ye, S. *Dalton Trans.* **2010**, 39 (3), 807–814.
- (41) Van de Heistee, B. J. J.; Schat, G.; Akkerman, O. S.; Bickelhaupt, F. *J. Organomet. Chem.* **1986**, 308 (1), 1–10.
- (42) Schock, L. E.; Marks, T. J. *J. Am. Chem. Soc.* **1988**, 110 (23), 7701.
- (43) Langer, J.; Kriek, S.; Fischer, R.; Görls, H.; Walther, D.; Westerhausen, M. *Organometallics* **2009**, 28 (19), 5814–5820.
- (44) Haneline, M. R.; Heyduk, A. F. *J. Am. Chem. Soc.* **2006**, 128 (26), 8410–8411.
- (45) Lee, H.; Bridgewater, B. M.; Parkin, G. *J. Chem. Soc. Dalton Trans.* **2000**, 24, 4490–4493.

- (46) Schock, L. E.; Brock, C. P.; Marks, T. J. *Organometallics* **1987**, *6* (2), 232–241.
- (47) Rong, Y.; Al-Harbi, A.; Parkin, G. *Organometallics* **2012**, *31* (23), 8208–8217.
- (48) Jantunen, K. C.; Scott, B. L.; Kiplinger, J. L. *J. Alloys Compd.* **2007**, *444–445*, 363–368.
- (49) Swenson, D. C.; Guo, Z.; Crowther, D. J.; Baenziger, N. C.; Jordan, R. F. *Acta Crystallogr. Sect. C Cryst. Struct. Commun.* **2000**, *56* (8), e313–e314.
- (50) Latesky, S. L.; McMullen, A. K.; Niccolai, G. P.; Rothwell, I. P.; Huffman, J. C. *Organometallics* **1985**, *4* (5), 902–908.
-